Beyond Neural Incompatibility: Cross-Scale Knowledge Transfer in Large Language Models through Latent Semantic Alignment

Anonymous ACL submission

Abstract

Large Language Models (LLMs) encode vast amounts of knowledge in their massive parameters, which is accessible to locate, trace, and analyze. Despite advances in neural interpretability, it is still not clear how to transfer knowledge in a fine-grained manner, namely parametric knowledge transfer (PKT). A key problem is enabling effective and efficient knowledge transfer across LLMs of different scales, which is essential for achieving greater flexibility and broader applicability in transferring knowledge between LLMs. Due to neural incompatibility, referring to the architectural and parametric differences between LLMs of varying scales, existing methods that directly reuse layer parameters are severely limited. In this paper, we identify the semantic alignment in latent space as the fundamental prerequisite for LLM cross-scale knowledge transfer. Instead of directly using the layer parameters, our approach takes activations as the medium of layer-wise knowledge transfer. Leveraging the semantics in latent space, our approach is simple and outperforms prior work, better aligning model behaviors across varying scales. Evaluations on four benchmarks demonstrate the efficacy of our method. Further analysis reveals the key factors easing cross-scale knowledge transfer and provides insights into the nature of latent semantic alignment.

1 Introduction

Language is the channel that lets humans and today's language models communicate, yet it throws away much of the fine detail that lives inside a model. When we teach a smaller model using instructions, explanations, or distilled datasets, we compress the source rich internal signals into text and lose structure that matters for behavior. A better way to transfer knowledge would move internal states directly, similar in spirit to the idea of brainwave communication where the sender shares what it is thinking rather than what it can say. Large language models make this idea practical because their parameters and hidden states are accessible. Prior work shows that we can analyze these internals, find where knowledge lives, and measure how specific parts influence predictions using attribution methods and information flow tools (Kokhlikyan et al., 2020; Yu and Ananiadou, 2024; Ferrando and Voita, 2024; Chen et al., 2025). This sets up our motivation for better knowledge transfer, where a target should be able to receive those signals directly from a source without going through text. It promises less loss, lower cost, and more truthful transfer.

We study this idea under parametric knowledge transfer. The goal is to move internal knowledge from a larger source to a smaller target so that the target acts more like the source. Prior work explores two routes in parameter space. Seeking extracts source parameters with sensitivity measures, injects them into the target through a LoRA initialization, and then relies on post alignment fine tuning (Zhong et al., 2024). LaTen aligns parameter spaces before injection using a light mapping to reduce the cost of later training (Tan et al., 2025). Both show that knowledge transfer is possible, but also report instability when the models differ in module design and parameter values, a gap described as *neural incompatibility* (Tan et al., 2025). In our analogy above, the "brainwave communication" corresponds to sharing layer outputs, not sharing layer parameters. We therefore treat activations as the medium of transfer and align semantics first, before any parameter updates.

We propose SEMALIGN, a semantics-first method for parametric knowledge transfer that uses layer outputs as the transfer signal. SemAlign consists of three steps: First, we run layer attribution on the source to locate layers that carry task relevant signal and we pair them with compatible layers in the target. This follows evidence that neuron

and concept relations are many to many and that robust layer selection matters (Yu and Ananiadou, 2024; Chen et al., 2025). Second, we align latent semantics for each paired layer. We decompose the source hidden states into semantic components in the source space and recombine them as supervisory hidden states in the target space. This treats aligned activations as supervision and follows results showing that shaping hidden states preserves meaning and supports stable adaptation (Gu et al., 2024, 2025; Kong et al., 2024). Third, we steer the target by optimizing the paired layers so that, on the same inputs, their outputs approach the aligned supervisory hidden states. In short, we align how layers behave rather than how weights look, which reduces neural incompatibility while keeping the procedure simple and efficient.

We evaluate SemAlign under the same setup as the prior work (Tan et al., 2025). We use four standard benchmarks on professional knowledge, mathematical reasoning and code generation. The experiments are conducted with Llama 2 models (Touvron et al., 2023), performing task related parametric knowledge transfer by pairing larger sources with smaller targets that differ in depth and width. Across all tasks, SemAlign improves target performance over task matched baselines and over parameter space transfer baselines. Two findings stand out: first, performing latent semantic alignment before any parameter update strongly predicts stable cross-scale transfer; second, steering a small set of paired layers is enough to induce broader behavioral alignment, which makes the method efficient in both compute and data. The replication repository is attached as supplementary material. To summarize, our contributions are as follows:

- We present a semantics-first view of parametric knowledge transfer for cross-scale language models. The formulation treats latent semantic alignment between paired layers as the prerequisite to transfer and uses layer outputs, not raw parameters, as the medium.
- We introduce SEMALIGN, which combines layer attribution and pairing, latent semantic alignment, and representation steering. This design addresses neural incompatibility that limits parameter space transfer in Seeking and LaTen (Zhong et al., 2024; Tan et al., 2025).
- We provide comprehensive experiments on extensive benchmarks with Llama 2. Results and analysis identify the key factors that ease cross-scale transfer and show consistent gains in the efficacy. We provide further discussion in the appendix.

2 Related Work

2.1 Knowledge Attribution in Language Models

Knowledge attribution studies methods for identifying where knowledge resides in large language models and how those components influence predictions. The focus has moved from layer level inspections to neuron level and path level analyses that scale to current models. One representative line designs a static, single pass neuron score that separates "query" and "value" neurons and avoids repeated gradient passes (Yu and Ananiadou, 2024). Moving from units to mechanisms, information flow routes rebuild prediction time computation as a sparse graph and show how influential parts work together during inference (Ferrando and Voita, 2024). In practical analyses, CAPTUM provides operators for layer and neuron attribution, including Internal Influence, Neuron Integrated Gradients, and DeepLIFT or SHAP, which many studies adopt as reproducible baselines (Kokhlikyan et al., 2020). Recent evidence also reports degenerate knowledge neurons, where different neuron sets encode the same fact; this observation supports concept aware or path aware selection when using attribution to guide editing or transfer (Chen et al., 2025).

2.2 Semantic Analysis and Latent Space Alignment

Semantic analysis and latent space alignment shape and match internal representations so that model adaptation preserves meaning rather than only optimizing an output loss. Within this view, a single research line proposes two connected methods that form a coherent pipeline. Vocabulary Defined Semantics (VDS) uses the model vocabulary to anchor directions in the hidden space and then clusters examples around these anchors, which stabilizes in context learning by better matching data to the model's internal semantic frame (Gu et al., 2024). Building on that foundation, Semantic Aware Layer Freezing (SALF) treats the structure exposed by VDS as semantic anchors at the layer level and freezes those parts while tuning the remainder, which preserves core semantics and works with parameter efficient finetuning and quan-

tization (Gu et al., 2025). A complementary research thread adjusts hidden states at test time with small edits, showing that behavior can be steered through representation space without heavy retraining (Kong et al., 2024).

2.3 Parametric Knowledge Transfer

Knowledge transfer includes source and target distillation, representational matching across layers, and parameter mixing through model merging or task vectors. These approaches provide strong baselines and tools, yet they often work in the output space or assume closely related architectures (Xu et al., 2024; Yang et al., 2024, 2025; Liu et al., 2024). Recent studies frame the problem as parametric knowledge transfer, where the goal is to move internal knowledge that lives inside a model, including parameters and intermediate computations such as activations and residual streams. A representative system, SEEKING, extracts sensitive components from a source, injects them into a target through LoRA initialization, and then applies post alignment fine tuning; results indicate that cross-scale transfer is feasible and that alignment quality is important for stability (Zhong et al., 2024). Follow up work on Neural Incompatibility examines alignment as the main bottleneck cross scales and distinguishes two design choices: PostPKT, which follows extract, inject, and train, and PrePKT, exemplified by LaTen, which aligns parametric spaces with light training before transfer (Tan et al., 2025). Our method adopts semantics-first plan by using latent semantic alignment as a precondition for parametric knowledge transfer, to mitigate neural incompatibility.

3 Motivational Analysis

3.1 Preliminary: Vocabulary-Defined Semantics

For the recognizable semantic meanings of a given LM, *vocabulary-defined semantics* proposed defining a set of special representations in the latent space to associate with the labels on the vocabulary. It quantifies the semantic property of LM latent space leveraging local isotropy (Cai et al., 2021), and benefits parameter optimizations, such as efficient logits computation (Gu et al., 2024). For each label on the LM vocabulary, there is an associated representation in the latent space, termed as "semantic basis", they share the same semantic meaning, as shown in Figure 1.

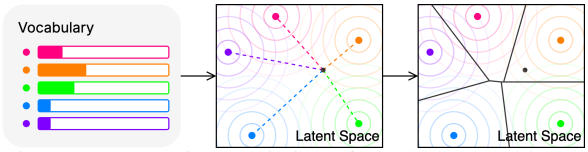

Figure 1: Semantic association of vocabulary and latent space. For each color label on the vocabulary (left), there is a color semantic basis in the latent space (middle). The semantics of the dark dot (indicating an arbitrary representation) in the latent space can be quantified as its cosine similarities to semantic bases. The semantics can be computed as probabilities on the vocabulary. When focusing on the nearest semantic basis for a given latent representation, a latent space can be quantified as discrete semantic regions (right).

For a given LM-head matrix, we conduct matrix multiplication to obtain semantic bases in the latent space. Since the computation direction is from logits to representations, instead of using the LM-head matrix $\mathbb{W}$, we use its pseudoinverse $\mathbb{W}^+$. If there are v labels in the vocabulary, there will be v unique semantic bases representing all semantic meanings. At the output side of LM, we multiply each onehot embedding $\vec{e}$ by the pseudoinverse matrix $\mathbb{W}^+$ to obtain the corresponding representation $\vec{s}$. That is, $\vec{s} = \vec{e} \cdot \mathbb{W}^+$. The computation is equivalent to solving the least squares problem of a system of linear equations. The time cost of computing semantic bases is rather low. For language models like LLaMA 2 (7B, 13B, and even 70B) which has 32k labels in the vocabulary, it takes around 10 seconds on an A100 GPU. Moreover, this is a one-time computation with persistent value.

3.2 Empirical Finding: Vector Nature of Semantics

Centered on each semantic basis, there forms a "semantic field". The concept of semantic field is similar to the *field* term in physics (such as electric field, then the semantic basis analogies to the electric pole). The semantics of an arbitrary latent representation can be quantified as the overlapping impact of multiple semantic fields, and further computed as probabilities (Gu et al., 2024). The process is "composition of semantics", where multiple *semantic components* become a *resultant vectors* via vector addition. We propose a hypothesis that the overlapping effects of semantic fields support a corresponding reversed operation "resolution of semantics". That is, a single *resultant vector* in latent space may be resolved into multiple *component vectors* along the directions of semantic bases.

In detail, for a given latent representation $\vec{r}$, its

semantic meaning can be projected to different semantic bases to obtain corresponding semantic components $\vec{c}_i = \texttt{proj}(\vec{r}, \vec{s}_i)$ (analogy to "component force" in a force field). By accumulating the decomposed semantics, we get a "resultant semantics" $\sum_{i=1}^{n} \vec{c}_i$ (analogy to "resultant force" in a force field). The equation $\vec{r} \parallel \sum_{i=1}^{n} \vec{c}_i$ stands approximately true. In contrast, when taking a random collection of vectors as semantic bases and obtain $\vec{c}_i = \texttt{proj}(\vec{r}, \vec{s}_i)$, the equation $\vec{r} \perp \sum_{i=1}^{n} \vec{c}_i$ stays true. It is consistent with the property of the latent space that, arbitrary vectors in a high-dimensional space tend to be orthogonal.

We conduct empirical experiments to validate the hypothesis. For a given data and LM, we first compute the outputs of each layer, and then decompose each layer outputs into semantic components and eventually recompose back as layer outputs. If the old layer outputs amd the new layer outputs share almost similar direction in the latent space, namely their cosine similarity is high, the hypothesis stands. We run with Qwen3 model on HumanEval, to study whether the hypothesis stand with the output-side semantic bases, and using input-side semantic bases for comparison. As shown in Figure 2, the hypothesis stand with the case of using output-side semantic bases because of the very high cosine similarities no matter the layer. In contrast, the situation of using input-side semantic bases is bad and the cosine similarities is close to zero, which indicates the common phenomenon in high-dimensional latent space that arbitrary vectors tend to be orthogonal to each other.

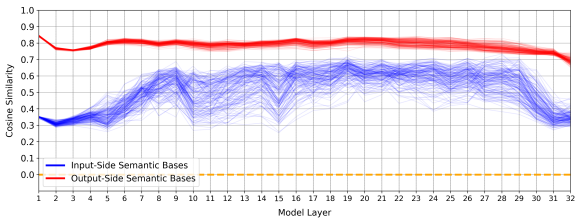

Figure 2: Empirical Validation of Semantics Decomposition on HumanEval with Llama2 (7B).

4 Approach

Our approach utilized LM semantics to align the latent space between certain layers of source and target models. The transferred knowledge by semantic alignment is layer outputs, as the supervisory signal for parameter optimization. We name our approach Semantic Alignment, short as SEMALIGN. The illustration of our approach is in Figure 3, and the main steps are: (1) First, we locate critical layers in source LM by attribution algorithm, and find the layer to pair in target LM by pairing strategy. The semantic alignment will happen between the pair layers, from source to target; (2) Then, we decompose the semantics of layer outputs in source latent space, and recompose as supervisory layer outputs in target latent space. It aligns latent spaces while preserving the semantics of layer outputs; (3) Further, in the target model, we optimize layer parameters using the supervisory layer outputs. For the same given data, the layer outputs of the paired layers become close, indicating the similar behaviors by source and target models.

4.1 Layer Attribution and Layer Pairing

Layer Attribution. We identify candidate source layers using *Layer Gradient* $\times$ *Activation* at the layer level: for each layer, we multiply the gradient of the supervised objective by the layer's activations and aggregate over tokens and channels to obtain a scalar importance score per layer. This choice is simple, stable, and available in standard attribution toolkits (Kokhlikyan et al., 2020).

Layer Pairing. Let the source have L_T layers and the target have L_S layers. We build a depth-aware mapping that assigns each target layer a source counterpart while preserving order. For target index $k \in \{1, \ldots, L_S\}$, define

$$\ell_k^{\mathrm{T}} = \max\left(1, \left\lfloor \frac{L_T}{L_S} k \right\rfloor\right) \in \{1, \ldots, L_T\},$$

which, for example, gives $\ell_k^{\mathrm{T}} = 2k$ when L_T=20 and L_S=10. This mapping is one-to-one when L_T/L_S is an integer; otherwise, some source layers may be shared across adjacent target layers. If a source layer $\ell_\star^{\mathrm{T}}$ is judged critical by attribution but does not coincide with any ℓ_k^{T}, we select the nearest *deeper-or-equal* target index

$$k^\dagger = \min\left\{ k' \in \{1, \ldots, L_S\} \;:\; \ell_{k'}^{\mathrm{T}} \geq \ell_\star^{\mathrm{T}} \right\},$$

defaulting to $k^\dagger$=L_S if the set is empty. We then operate on the pair $(\ell_{k^\dagger}^{\mathrm{T}}, k^\dagger)$, which preserves depth order and guarantees a concrete target partner for every attributed source layer.

If supervision requires a target at an exact target depth while L_T/L_S is non-integer, we interpolate

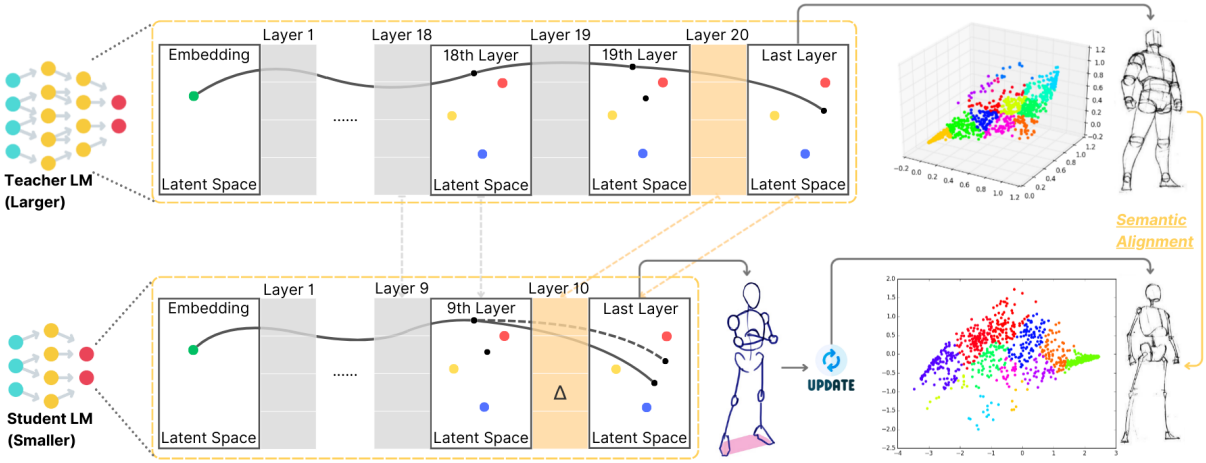

Figure 3: Illustration of our cross-scale knowledge transfer approach. Assume a 20-layer source LM and a 10-layer target LM, then: (1) model layers in source and target LMs are pairs by dashed arrow lines. Marked by orange color, the 20th source layer is located as critical, and its pair is the 10th target layer, namely the layer to optimize; (2) represented by the dots in 3D and 2D spaces, the layer outputs from source model are decomposed in the larger dimensional source latent space and recomposed in the smaller dimensional target latent space, as the supervisory signal. It undergos dimensional reduction but still preserves complete semantics, represented by the changes to gray bots, remaining the body gesture but reducing details; (3) the paired target layer will be updated, to make the target layer outputs be close to the supervisory signal. It is similar to blue bots, to be adjusted playing the same body gesture as gray bots does. Afte the cross-scale knowledge transfer, target layer outputs will steer to the supervisory signal, represented by the dashed curve, and partial layer parameters are optimized, marked by the delta symbol. In the last layer's latent space, the outputs is represented by the small dark dot whose distances to big color dots indicates the probabilities in LM vocabulary. For source LM, its dark dot is close to the red dot, so its output label is the corresponding red label; while for target LM, its output label was the corresponding blue but will become red after knowledge transfer, since its dark dot moves far away from the blue dot while approaching the red dot.

between adjacent source layers. Let the target depth be $k^\dagger$ and set $\rho = k^\dagger / L_S$. Define $u = L_T \rho$, then

$$
\begin{aligned}
a &= \max\big(1,\, \min(\lfloor u \rfloor,\, L_T - 1)\big), \\
b &= a + 1, \\
\lambda &= \mathrm{clip}(u - a,\, 0,\, 1).
\end{aligned}
$$

Given source representations $\mathbf{h}^{\mathrm{T}}_{(a)}$ and $\mathbf{h}^{\mathrm{T}}_{(b)}$ at the supervision interface, the interpolated target for target layer $k^\dagger$ is

$$
\tilde{\mathbf{h}}^{\mathrm{T}} = (1 - \lambda)\, \mathbf{h}^{\mathrm{T}}_{(a)} \;+\; \lambda\, \mathbf{h}^{\mathrm{T}}_{(b)}.
$$

This yields a well-defined supervisory signal from the source for every target depth while respecting layer ordering.

4.2 Latent Semantic Alignment (from Source LM to Target LM)

We construct a training-free, semantics-preserving mapping from a *source* layer's latent space to a *target* layer's latent space. The source and target come from the same LM family at different scales, and their semantic bases are index-aligned (Section Preliminaries). The idea is to *decompose* the source vector into components along source semantic atoms and *recompose* those components in the target basis using the *same* coefficients.

Let $\mathbf{h}^{\mathrm{T}} \in \mathbb{R}^{D_T}$ be a source-layer output at the supervision interface and $\mathbf{h}^{\mathrm{S}} \in \mathbb{R}^{D_S}$ a target-layer vector (to be constructed as a target). Let $S_{\mathrm{T}} = [\mathbf{s}^{\mathrm{T}}_1, \ldots, \mathbf{s}^{\mathrm{T}}_m] \in \mathbb{R}^{D_T \times m}$ and $S_{\mathrm{S}} = [\mathbf{s}^{\mathrm{S}}_1, \ldots, \mathbf{s}^{\mathrm{S}}_m] \in \mathbb{R}^{D_S \times m}$ denote the source and target semantic bases, respectively, with column i in S_{T} and S_{S} referring to the same semantic atom. Assume unit-normalized columns: $\|\mathbf{s}^{\mathrm{T}}_i\|_2 = \|\mathbf{s}^{\mathrm{S}}_i\|_2 = 1$.

Semantics-preserving Decomposition and Recomposition We form *semantic coefficients* by cosine projection in the source space:

$$
\begin{aligned}
\mathbf{a} &= \big[\cos(\mathbf{h}^{\mathrm{T}}, \mathbf{s}^{\mathrm{T}}_1), \ldots, \cos(\mathbf{h}^{\mathrm{T}}, \mathbf{s}^{\mathrm{T}}_m)\big]^\top \\
&= \frac{S_{\mathrm{T}}^\top \mathbf{h}^{\mathrm{T}}}{\|\mathbf{h}^{\mathrm{T}}\|_2} \;\in \mathbb{R}^m.
\end{aligned} \tag{1}
$$

We then *recompose* in the target space with the same coefficients:

$$
\tilde{\mathbf{h}}^{\mathrm{S}} \;=\; S_{\mathrm{S}}\, \mathbf{a} \;\in \mathbb{R}^{D_S}. \tag{2}
$$

The vector $\tilde{\mathbf{h}}^{\mathrm{S}}$ serves as the supervisory signal for the target layer output at the same interface.

Because column i of S_{T} and S_{S} denote the same semantic atom and all columns are unit-norm, the pair $\big($decompose in source: $\mathbf{a} = S_{\mathrm{T}}^{\top}\mathbf{h}^{\mathrm{T}}/\|\mathbf{h}^{\mathrm{T}}\|_2$, recompose in target: $\tilde{\mathbf{h}}^{\mathrm{S}} = S_{\mathrm{S}}\mathbf{a}\big)$ transfers an identical set of component weights from source to target. Thus, the semantic content is preserved; only the ambient basis changes.

4.3 Cosine-Only Layer and Output Alignment

We adapt the target by updating only the parameters of its paired layer k while freezing all others. The training objective consists of *two* cosine-alignment terms with no additional weights: (i) a *layer-level* cosine loss that aligns the k-th layer's activations to the semantics-preserving target, and (ii) an *output-level* cosine loss that aligns the final-layer logits to the supervised label direction. This naming emphasizes that both the intermediate representation (for semantic alignment) and the model output (a geometric surrogate of cross-entropy) are optimized using cosine similarity alone.

Let $\theta^{(k)}$ denotes the parameters of target layer k. Let $\mathbf{h}^{(k)} \in \mathbb{R}^{B\times T\times D}$ be the target activations at a fixed supervision interface, chosen as the sublayer output *before* residual addition. Let $\mathbf{h}_{\star}^{(k)} \in \mathbb{R}^{B\times T\times D}$ be the semantics-preserving target instantiated at the same interface (broadcast across batch/tokens as appropriate). Let $\mathbf{z} \in \mathbb{R}^{B\times T\times|\mathcal{Y}|}$ be the final-layer logits, and let $\mathbf{y}^{\mathrm{oh}} \in \{0,1\}^{B\times T\times|\mathcal{Y}|}$ be one-hot (or label-smoothed) target distributions over $\mathcal{Y}$.[1]

The total training objective is an unweighted sum of these two terms: $\mathcal{L}(\theta^{(k)}) = \mathcal{L}_{\mathrm{layer}} + \mathcal{L}_{\mathrm{out}}$. The first term $\mathcal{L}_{\mathrm{layer}} = 1 - \mathrm{Avg}\Big[\cos\big(\mathbf{h}^{(k)}, \mathbf{h}_{\star}^{(k)}\big)\Big]$ represents the targeted layer's alignment (semantic alignment at layer k); while the second term $\mathcal{L}_{\mathrm{out}} = 1 - \mathrm{Avg}\big[\cos\big(\mathbf{z}, \mathbf{y}^{\mathrm{oh}}\big)\big]$ represents the last layer's alignment (geometric surrogate of CE at the last layer). Besides, $\mathrm{Avg}[\cdot]$ denotes a simple average over supervised positions, and $\cos(\mathbf{u},\mathbf{v}) = \dfrac{\langle \mathbf{u},\mathbf{v}\rangle}{\|\mathbf{u}\|_2\,\|\mathbf{v}\|_2}$.

The first term, $\mathcal{L}_{\mathrm{layer}}$, enforces *latent semantic alignment*: it drives the k-th layer's representation toward the semantics-preserving target constructed by decomposing the source output into source semantic components and recomposing them in the target basis. The second term, $\mathcal{L}_{\mathrm{out}}$, aligns the final logits with the ground-truth direction in label space; because cosine similarity is scale-invariant in the logit space, this term acts as a principled geometric surrogate for cross-entropy, encouraging the model to place probability mass on the correct label while avoiding sensitivity to logit scale. Together, the two cosine objectives couple representation-level semantics with output-level correctness using a single, consistent geometric criterion.

We backpropagate through the full network but update only $\theta^{(k)}$. The target $\mathbf{h}_{\star}^{(k)}$ and the label vectors $\mathbf{y}^{\mathrm{oh}}$ are treated as constants. Matching the supervision interface for $\mathbf{h}^{(k)}$ and $\mathbf{h}_{\star}^{(k)}$ (both pre-residual) ensures that the alignment term acts directly on the representation controlled by layer k, while the output cosine term refines the model's decision geometry at the final layer.

5 Experiments

In the experiments, we mainly study how our approach performs in parameteric knowledge transfer comparing with PKT baselines. We also conduct analysis based on the latent representation similarities between source and target models before and after latent semantic alignment.

5.1 Setup

Datasets. We use four well-established benchmarks, covering the most common downstream tasks: MMLU measures professional knowledge (Hendrycks et al., 2021); GSM8K measures mathematical reasoning (Cobbe et al., 2021); HumanEval and MBPP measure code generation (Chen et al., 2021; Austin et al., 2021).

Models. We conduct experiments with Llama 2 (Touvron et al., 2023) models, mainly chat versions instead of base versions for the better instruction-following ability. Besides, we employ LM variants to study the transfer from further-finetuned source models to a same target model, CodeLlama-13B-Python (Roziere et al., 2023) and WizardCoder-13B-Python (Luo et al., 2023). They are finetuned on Llama-2-13B with massive code data for an enhanced coding performance.

Metrics. For MMLU and GSM8K, we calculate *accuracy* in zero-shot setting; and for HumanEval and MBPP, we calculate *pass@1*. Larger scores mean better performance.

Baselines. The prior work on parametric knowledge transfer is SEEKING and LATEN, which are

[1] For instance-level tasks, use per-example logits $\mathbf{z} \in \mathbb{R}^{B\times|\mathcal{Y}|}$ and one-hot target $\mathbf{y}^{\mathrm{oh}} \in \{0,1\}^{B\times|\mathcal{Y}|}$.

the baselines in our experiments. Both perform parametric knowledge transfer in two stages: Seeking is PostPKT (inject-then-train) while LaTen is PrePKT (align-then-inject). SEEKING first *extracts* task-relevant parameters from a source by ranking weights via sensitivity scores (gradient×parameter on a seed set), then *injects* them into a target. Layer-wise importance is aggregated to pick the top layers; within each selected matrix, a high-sensitivity sub-block is chosen to bridge width/depth gaps. Each extracted block is SVD-factorized to initialize a low-rank LoRA (B, A), after which the target is post-aligned by standard fine-tuning. LATEN adopts a *Locate-Then-Align* pipeline to minimize post-training. It *locates* neuron-level carriers of knowledge in FFN/MHSA using static attribution, selects top neurons per layer, and forms source-side deltas. A lightweight hypernetwork g_ϕ is trained on a tiny alignment set to *pre-align* these deltas into the target parameter shape/scale, which are then injected once for immediate gains. This design targets cross-model incompatibilities by aligning deltas before injection rather than SVD-to-LoRA initialization plus post-alignment.

5.2 Results

Cross-Scale Knowledge Transfer. In all of four benchmarks, SEMALIGN improves substantially over Llama2-7B-Chat while remaining below the Llama2-13B-Chat source, and it stays closer to the source than the other transfer baselines on average. Concretely, the absolute gaps between SemAlign and 13B are 2.60 (MMLU: 50.30 vs 52.90), 1.34 (GSM8K: 19.21 vs 20.55), 1.41 (HumanEval: 17.34 vs 18.75), and 0.42 (MBPP: 18.78 vs 19.20), averaging 1.44 points. This average gap is smaller than SEEKING (≈ 3.92) and LATEN (≈ 3.43). A per-task view shows one exception—on GSM8K, LaTen (20.47) is numerically closest to 13B (20.55)—while SEEKING overshoots the source (28.23). Overall, SemAlign's three-of-four closer margins indicate it learns the source behavior more faithfully than the baselines.

Models	MMLU	GSM8K	HumanEval	MBPP
Llama2-7B-Chat	44.20	16.07	14.05	17.80
Llama2-13B-Chat	52.90	20.55	18.75	19.20
Seeking	49.60	**28.23**	15.44	**20.60**
LaTen	44.40	20.47	14.63	18.20
SemAlign	**50.30**	19.21	**17.34**	18.78

Table 1: Results of Parametric Knowledge Transfer in Diverse Downstream Tasks.

On task leadership, SemAlign attains the best transferred performance on MMLU (50.30) and HumanEval (17.34), surpassing both Seeking (49.60, 15.44) and LATEN (44.40, 14.63), whereas SEEKING leads on GSM8K (28.23) and MBPP (20.60). Notably, SEEKING exceeds the 13B source on both GSM8K (+7.68) and MBPP (+1.40), while SemAlign remains below but close to the source; this pattern is consistent with SemAlign's cosine-similarity objective encouraging conservative matching of source representations, whereas SEEKING appears to incorporate additional parameter optimization beyond pure transfer.

There shows an observation that, the trade-off between stability and aggressiveness across methods. SEEKING achieves large gains on reasoning- and coding-flavored datasets by overshooting the source (GSM8K, MBPP), suggesting stronger task-specific optimization, while SemAlign stays within ≤ 2.60 points of the source on every task, indicating steadier transfer that narrows the gap without over-amplifying particular skills.

Knowledge Transfer from Finetuned Models. In five of six source–task settings, SEMALIGN consistently outperforms the transfer baselines, indicating stronger parametric knowledge transfer. With Llama2-13B-Chat as source, it leads LATEN and SEEKING on HumanEval (17.34 vs 14.63/15.44), and only trails SEEKING on MBPP (18.78 vs 20.60). The advantage becomes clearer with code-specialized sources: from CodeLlama-13B-Python, SemAlign reaches 20.12 (+4.07 over SEEKING, +6.10 over LATEN) on HumanEval and 22.35 (+0.95, +4.55) on MBPP; from WizardCoder-13B-Python, it attains 19.46 (+4.42, +5.44) and 21.18 (+1.38, +2.58) on HumanEval and MBPP, respectively. These trends show that SemAlign extracts and transfers source competency more reliably, especially when the source is stronger in coding.

Across two coding benchmarks, all methods remain far below the finetuned sources (CodeLlama-13B-Python: 47.56/37.80; WizardCoder-13B-Python: 56.71/41.60), despite often surpassing Llama2-7B-Chat and sometimes even matching or exceeding Llama2-13B-Chat (e.g., SEEKING on MBPP with 20.60 vs 19.20). This gap suggests that the extensive, task-specific optimization baked into code-specialized sources is difficult to reconstruct via short-horizon transfer; objectives like cosine matching encourage conservative alignment

Models	HumanEval	MBPP
Llama2-7B-Chat	14.05	17.80
Llama2-13B-Chat	18.75	19.20
Seeking	15.44	**20.60**
LaTen	14.63	18.20
SemAlign	**17.34**	18.78
CodeLlama-13B-Python	47.56	37.80
Seeking	16.05	21.40
LaTen	14.02	17.80
SemAlign	**20.12**	**22.35**
WizardCoder-13B-Python	56.71	41.60
Seeking	15.04	19.80
LaTen	14.02	18.60
SemAlign	**19.46**	**21.18**

Table 2: Results Parametric Knowledge Transfer from Finetuned source Models.

to source representations rather than aggressive task re-optimization, limiting the attainable ceiling without longer or more targeted finetuning.

An additional observation is that SEEKING only overshoots the source on MBPP when the source is the generalist Llama2-13B-Chat (20.60 $>$ 19.20) but not when the source is code-specialized; meanwhile, SEMALIGN shows its largest margins over baselines precisely when transferring from code-specialized sources. This pattern hints that aggressive, task-specific optimization in SEEKING can exploit headroom left by generalist sources, whereas SemAlign's representation-faithful transfer scales better with source specialization.

5.3 Analysis

We adopt Centered Kernel Alignment (CKA) (Kornblith et al., 2019) as the analysis tool to study the similarities between layer outputs from source and target models. We run Llama2-chat models on HumanEval data. CKA is commonly used to compute the similarities between feature representations in neural networks, which is based on Hilbert-Schmidt Independence Criterion (HSIC).

As shown in Figure 4, there are high similarities between the layer outputs from source and target models, especially along the main diagonal. It indicates that, there exists no neuron incompatibility if using layer outputs as the medium of parameteric knowledge transfer, instead of directly using layer parameters. The highest similarities is almostly layer-by-layer, from shallow to deep. Meanwhile, the cases before (the left subfigure) and after (the right subfigure) latent semantic alignment share very similar pattern of similarities. It means, adopting latent space alignment is a safe way to utilize the similarities between layer outputs between cross-scale language models.

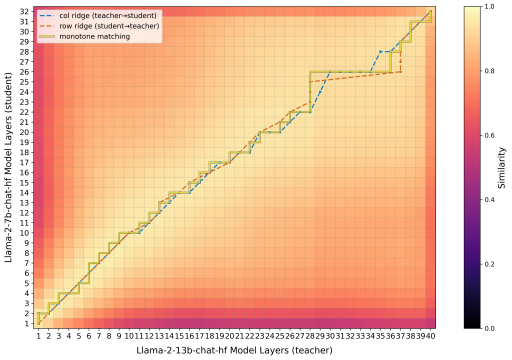

(a) source-target w/o alignment

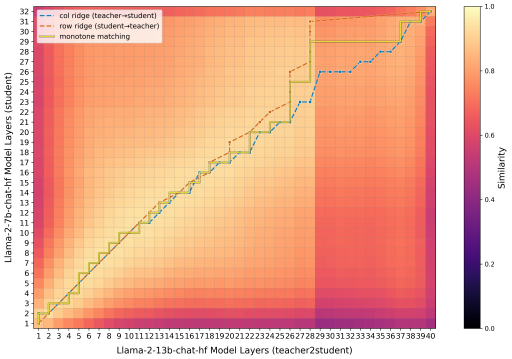

(b) source-target w/ alignment

Figure 4: Comparison of Layer-wise Representation Similarities between LLMs.

6 Conclusion

We studied parametric knowledge transfer across differently scaled LLMs from a *semantics-first* perspective. Rather than moving raw parameters as in prior paradigms, we use layer outputs as the medium of transfer and identify *latent semantic alignment* as the prerequisite for stable cross-scale transfer. Building on this view, SEMALIGN locates and pairs source and target layers, aligns their latent semantics, and then steers the target so its paired layers reproduce the aligned supervisory hidden states. This design avoids neural incompatibility, simplifies the procedure, and makes transfer efficient in both compute and data. Empirically, SemAlign improves targets over task-matched baselines and over parameter-space transfer methods on four benchmarks with Llama 2 families. The results support our central claim: treating activations as the carrier of knowledge and aligning semantics-first provides a robust path to cross-scale PKT.

Limitations

Our evaluation is limited in scope. The experiments are on four benchmarks and mainly study transfer within the Llama 2 family across scales, with a few further-finetuned variants. It is still not clear how well SemAlign works for more diverse settings, such as other model families with different tokenizers or architectures, longer-context use, multilingual tasks, or safety-critical behavior.

SemAlign further assumes that the source and target share a usable semantic correspondence, so that we can decompose a representation in the source and recompose it in the target. When this correspondence is weak (such as vocabulary mismatch or semantic drift), the alignment signal can be noisy and transfer may degrade. More broadly, we use a cosine-only objective and lightweight updates to keep training stable. This choice can cap the best achievable performance, and it does not fully prevent interference with other skills.

References

Zeyuan Allen-Zhu and Yuanzhi Li. Physics of language models: Part 3.3, knowledge capacity scaling laws. In *The Thirteenth International Conference on Learning Representations*.

Jacob Austin, Augustus Odena, Maxwell Nye, Maarten Bosma, Henryk Michalewski, David Dohan, Ellen Jiang, Carrie Cai, Michael Terry, Quoc Le, and 1 others. 2021. Program synthesis with large language models. *arXiv preprint arXiv:2108.07732*.

Xingyu Cai, Jiaji Huang, Yu-Lan Bian, and Kenneth Ward Church. 2021. Isotropy in the contextual embedding space: Clusters and manifolds. In *International Conference on Learning Representations*.

Mark Chen, Jerry Tworek, Heewoo Jun, Qiming Yuan, Henrique Ponde De Oliveira Pinto, Jared Kaplan, Harri Edwards, Yuri Burda, Nicholas Joseph, Greg Brockman, and 1 others. 2021. Evaluating large language models trained on code. *arXiv preprint arXiv:2107.03374*.

Yuheng Chen, Pengfei Cao, Yubo Chen, Yining Wang, Shengping Liu, Kang Liu, and Jun Zhao. 2025. Cracking factual knowledge: A comprehensive analysis of degenerate knowledge neurons in large language models. In *Proceedings of ACL 2025*.

Karl Cobbe, Vineet Kosaraju, Mohammad Bavarian, Mark Chen, Heewoo Jun, Lukasz Kaiser, Matthias Plappert, Jerry Tworek, Jacob Hilton, Reiichiro Nakano, and 1 others. 2021. Training verifiers to solve math word problems. *arXiv preprint arXiv:2110.14168*.

Javier Ferrando and Elena Voita. 2024. Information flow routes: Automatically interpreting language models at scale. In *Proceedings of EMNLP 2024*.

Jian Gu, Aldeida Aleti, Chunyang Chen, and Hongyu Zhang. 2024. Vocabulary-defined semantics: Latent space clustering for improving in-context learning. *arXiv preprint arXiv:2401.16184*.

Jian Gu, Aldeida Aleti, Chunyang Chen, and Hongyu Zhang. 2025. A semantic-aware layer-freezing approach to computation-efficient fine-tuning of language models. In *Findings of the Association for Computational Linguistics: ACL 2025*.

Dan Hendrycks, Collin Burns, Saurav Kadavath, Akul Arora, Steven Basart, Eric Tang, Dawn Song, and Jacob Steinhardt. 2021. Measuring mathematical problem solving with the math dataset. *arXiv preprint arXiv:2103.03874*.

Narine Kokhlikyan, Vivek Miglani, Miguel Martin, Edward Wang, Bilal Alsallakh, Jonathan Reynolds, Alexander Melnikov, Natalia Kliushkina, Carlos Araya, Siqi Yan, and Orion Reblitz-Richardson. 2020. Captum: A unified and generic model interpretability library for pytorch. *Preprint*, arXiv:2009.07896.

Lingkai Kong and 1 others. 2024. Aligning large language models with representation editing. In *Advances in Neural Information Processing Systems 37 (NeurIPS 2024)*.

Simon Kornblith, Mohammad Norouzi, Honglak Lee, and Geoffrey Hinton. 2019. Similarity of neural network representations revisited. In *International conference on machine learning*, pages 3519–3529. PMlR.

Woosuk Kwon, Zhuohan Li, Siyuan Zhuang, Ying Sheng, Lianmin Zheng, Cody Hao Yu, Joseph E. Gonzalez, Hao Zhang, and Ion Stoica. 2023. Efficient memory management for large language model serving with pagedattention. In *Proceedings of the ACM SIGOPS 29th Symposium on Operating Systems Principles*.

Ziyue Liu and 1 others. 2024. Model merging in llms, mllms, and beyond: Methods, theories, applications, and opportunities. *arXiv preprint arXiv:2408.07666*.

Ziyang Luo, Can Xu, Pu Zhao, Qingfeng Sun, Xiubo Geng, Wenxiang Hu, Chongyang Tao, Jing Ma, Qingwei Lin, and Daxin Jiang. 2023. Wizardcoder: Empowering code large language models with evol-instruct. *arXiv preprint arXiv:2306.08568*.

Adam Paszke, Sam Gross, Francisco Massa, Adam Lerer, James Bradbury, Gregory Chanan, Trevor Killeen, Zeming Lin, Natalia Gimelshein, Luca Antiga, Alban Desmaison, Andreas Köpf, Edward Yang, Zach DeVito, Martin Raison, Alykhan Tejani, Sasank Chilamkurthy, Benoit Steiner, Lu Fang, and 2 others. 2019. Pytorch: An imperative style, high-performance deep learning library. In *Neural Information Processing Systems*.

Baptiste Roziere, Jonas Gehring, Fabian Gloeckle, Sten Sootla, Itai Gat, Xiaoqing Ellen Tan, Yossi Adi, Jingyu Liu, Romain Sauvestre, Tal Remez, and 1 others. 2023. Code llama: Open foundation models for code. *arXiv preprint arXiv:2308.12950*.

Yuqiao Tan, Shizhu He, Kang Liu, and Jun Zhao. 2025. Neural incompatibility: The unbridgeable gap of cross-scale parametric knowledge transfer in large language models. In *Proceedings of the 63rd Annual Meeting of the Association for Computational Linguistics (Long Papers)*, pages 21586–21601.

Hugo Touvron, Thibaut Lavril, Gautier Izacard, Xavier Martinet, Marie-Anne Lachaux, Timothée Lacroix, Baptiste Rozière, Naman Goyal, Eric Hambro, Faisal Azhar, and 1 others. 2023. Llama: Open and efficient foundation language models. *arXiv preprint arXiv:2302.13971*.

Thomas Wolf, Lysandre Debut, Victor Sanh, Julien Chaumond, Clement Delangue, Anthony Moi, Pierric Cistac, Tim Rault, Rémi Louf, Morgan Funtowicz, and Jamie Brew. 2019. Transformers: State-of-the-art natural language processing. In *Conference on Empirical Methods in Natural Language Processing*.

Xiaohan Xu, Ming Li, Chongyang Tao, Tao Shen, Reynold Cheng, Jinyang Li, Can Xu, Dacheng Tao, and Tianyi Zhou. 2024. A survey on knowledge distillation of large language models. *arXiv preprint arXiv:2402.13116*.

Chuanpeng Yang, Wang Lu, Yao Zhu, Yidong Wang, Qian Chen, Chenlong Gao, Bingjie Yan, and Yiqiang Chen. 2024. Survey on knowledge distillation for large language models: Methods, evaluation, and application. *arXiv preprint arXiv:2407.01885*.

Enneng Yang and 1 others. 2025. A review of model merging approaches. *arXiv preprint arXiv:2503.08998*.

Zeping Yu and Sophia Ananiadou. 2024. Neuron-level knowledge attribution in large language models. In *Proceedings of the 2024 Conference on Empirical Methods in Natural Language Processing*.

Ming Zhong, Chenxin An, Weizhu Chen, Jiawei Han, and Pengcheng He. 2024. Seeking neural nuggets: Knowledge transfer in large language models from a parametric perspective. In *Proceedings of the International Conference on Learning Representations (ICLR)*.

A Implementation Details

A.1 Stats of Language Models

The stats of language models in our experiments are shown in Table 3.

	Llama2		CodeLlama	WizardCoder
	7B	13B	13B	13B
Head Num.	32	40	40	40
Layer Num.	32	40	40	40
Dimension	4,096	5,120	5,120	5,120
Vocabulary	32,000	32,000	32,000	32,001

Table 3: Stats of Llama 2 Language Models.

A.2 Implementations Details

We follow the experimental protocol of LaTen for a fair comparison, but unlike LaTen, our approach uses a single training phase only: the alignment operation is integrated into the training objective as an auxiliary loss term, with no separate alignment stage or post-training optimization. In detail, we fine-tune the smaller model for 5 epochs with a batch size of 64 and a learning rate of 3×10^{-4} (for HumanEval, 3×10^{-5}), and use 3 epochs in the SFT setting; LoRA uses rank r=16 and is inserted into FFN (`up_proj`, `down_proj`) and MHSA (`v_proj`, `o_proj`) modules. For baseline reproduction under LaTen's protocol, the hypernetwork is trained with a learning rate of 1×10^{-5} and weight decay 0.05, the sample size is P=16, and 10% of neurons are transferred per layer. The hyperparameters on alignment and trainment are shown in Table 4 and Table 5. The experiments are conducted via a single run, with the global random-seed 42.

Our implementation uses deep learning framework PyTorch (Paszke et al., 2019), Transformers (Wolf et al., 2019) and vLLM (Kwon et al., 2023).

	MMLU	GSM8K	HumanEval	MBPP
Steps	2	4	3	8
Align Size	32	64	48	128
Learning Rate	3e-5	3e-5	3e-5	3e-5

Table 4: Implementation Details in Alignment.

	MMLU	GSM8K	HumanEval	MBPP
Epochs	5	5	3	5
Train Size	1000	1000	1000	300
Learning Rate	3e-4	3e-4	3e-5	3e-4

Table 5: Implementation Details in Training.

A.3 AI Use Disclosure

We use a business LLM (GPT-5 [2]) to merely aid or polish our paper writing.

[2] https://openai.com/gpt-5/

B Details of Parametric Knowledge Transfer Baselines

Both baselines view knowledge as model weights and use the same two-step process: *extract* from the source, then *inject* into the target. They also handle layer/width mismatches and are tested on multiple LLM benchmarks. SEEKING focuses on sensitivity-based selection and LoRA initialization, followed by post-training alignment, so its alignment cost comes after injection but yields stable gains. LATEN focuses on neuron-level localization and hypernetwork pre-alignment, shifting the cost upfront to reduce or avoid post-training; in doing so, it highlights neural incompatibility and motivates semantics-first alignment. The detailed technical descriptions are as follows:

B.1 Illustrate SEEKING

SEEKING treats parametric knowledge transfer as two stages: *extract* task-related parameters from a larger source, then *inject* them into a smaller target and perform *post-alignment* fine-tuning. Given a task $\mathcal{T}$ and a small *seed* set produced by the source (typically a few dozen decoded examples), SEEKING assigns an importance score to each source parameter θ_i via *sensitivity*:

$$S_{i,j}^{\mathcal{T}} = \left|\theta_i^\top \nabla_{\theta_i} \mathcal{L}\big(x_j^{\mathcal{T}}, y_j^{\mathcal{T}} \,|\, \Theta\big)\right|,$$
$$S_i^{\mathcal{T}} = \sum_{j=1}^{k} S_{i,j}^{\mathcal{T}}.$$

a first-order approximation of the loss increase if θ_i were removed. Layer scores are obtained by summing parameter sensitivities within the layer; the top L_s layers (order-preserving) are kept for transfer. To bridge depth/width mismatches, SEEKING performs *sensitivity-guided dimensionality reduction* on each selected weight matrix $W^l \in \mathbb{R}^{n_l \times m_l}$ by choosing a submatrix $W^l_{\text{extract}} \in \mathbb{R}^{n_s \times m_s}$ (rows/columns or 2D block) that maximizes cumulative sensitivity:

$$W^l_{\text{extract}} = \arg\max_{W' \subseteq W^l} \sum_{\theta_i \in W'} S_i \quad \text{s.t.} \quad n_s \le n_l,\ m_s \le m_l.$$

The extracted blocks across layers are aggregated into $\Delta\Theta_{\text{extract}}$. For *injection*, each W^l_{extract} is factorized with SVD, $U\Sigma V^\top$, to initialize a rank-r LoRA pair (B, A) via $B \leftarrow U_{[:,1:r]}\Sigma_{1:r,1:r}$ and $A \leftarrow V^\top_{1:r,:}$, yielding an initialized target

$$W^{l\star} = W^l - W^l_{\text{extract}} + BA,$$

after which the target is fine-tuned to align the injected deltas. Empirically, SEEKING reports consistent gains across reasoning, professional knowledge, instruction-following, and open-domain dialogue, and analyzes factors such as source scale, initialization strategy, seed count, module origin, and LoRA rank.

B.2 Illustrate LATEN

LATEN formalizes two PKT regimes: *PostPKT* (inject then train-to-align) and *PrePKT* (align then inject). It proposes *Locate-Then-Align* to reduce or avoid post-training. For a larger source M_ℓ with parameters Θ_ℓ and a smaller target M_s with Θ_s, LaTen first *locates* the most informative sites at *neuron* granularity, then learns a light *hypernetwork* to *pre-align* source deltas to the target parameter space before injection:

$$\begin{aligned} \Delta\Theta_\ell &\leftarrow \mathrm{Locate}(M_\ell; \mathcal{D}_{\text{extract}}), \\ \widehat{\Delta\Theta}_s &\leftarrow g_\phi(\Delta\Theta_\ell), \\ \Theta_s^\star &\leftarrow \mathrm{Inject}(\Theta_s, \widehat{\Delta\Theta}_s). \end{aligned}$$

Using a static neuron-level attribution method, LaTen scores neurons in both FFN and MHSA (per selected layer; last-useful-token based) and selects the top-k neurons per layer for transfer, motivated by evidence that neurons serve as units storing skills/knowledge; this yields vectorized source deltas $\Delta\Theta_\ell$ over chosen FFN/MHSA submodules.

To bridge the width/depth gaps and value-scale discrepancies, a small two-layer MLP *hypernetwork* g_ϕ (with ReLU) is trained on a tiny *alignment* set (often < 100 examples) to map source deltas into target-shaped deltas by minimizing the LM loss while the base weights remain frozen:

$$\min_\phi \ \mathbb{E}_{(x,y)\in\mathcal{D}_{\text{align}}} \mathcal{L}_{\text{LM}}\big(y;\ M_s(x;\ \Theta_s \oplus g_\phi(\Delta\Theta_\ell))\big).$$

After learning g_ϕ, $\widehat{\Delta\Theta}_s$ is injected once, aiming for immediate gains without further training. LaTen contrasts this with SEEKING's SVD-to-LoRA initialization, and attributes transfer instability to *neural incompatibility* (low similarity across behavioral and parametric spaces) when deltas are unaligned. Experiments show promising (though not uniformly stable) improvements under PrePKT and comparisons against baselines such as self-derived LoRA and language-based distillation.

C Discussion

C.1 Medium in Parametric Knowledge Transfer

Compare with the prior work such as Seeking and LaTen, which take model weights as the medium for knowledge transfer, SEMALIGN suggest using layer outputs as the medium. Our approach shows advantages in efficacy, and also, requires almost no computation cost for alignment. Moreover, our methodology have theorically better performance based on the following reasons.

For the perspective of information transfer, layer outputs as the medium requires less bandwidth than the prior work of PKT, as well as the general knowledge transfer work. Because in language models, the dimension size of layer outputs is much smaller than that of layer parameters, as well as that of the probabilities in LM vocabulary. A smaller size indicates less information to transfer. Therefore, transferring more knowledge of same quality requires more computation cost; or, transferring more knowledge by costing same computation indicates high information loss.

From the perspective of the association between knowledge and neurons, layer outputs is a better choice than layer parameters. It is known by prior work that LM knowledge and neurons follow many-to-many dynamic associations (Allen-Zhu and Li). Therefore, if knowledge transfer is conducted through layer parameters (especially LaTen), certain target parameters will be updated with certain source parameters. However, no matter the layer parameters from the source or target model, they associate with not only the current given data, but also other data. Such practice of parametric knowledge transfer by direct parameter manipulation is likely to cause potential side effects. In contrast, Seeking indicates a safer practice, which introduces the idea of parametric knowledge transfer to the framework of parameter-efficient finetuning.

C.2 Limitations and Future Work

Our study focuses on a limited set of tasks, and layer-level pairing, while broader coverage (architectures, modalities, safety-critical settings) remains open. Future directions include: (1) extending semantic alignment to finer granularity (sub-layer, attention head) (2) comparing objectives that combine causal and semantic constraints; (3) exploring better strategies on layer pairing based on the layer outputs in source and target models; (4) scaling analyses across families with larger architectural gaps to stress-test robustness. We hope SemAlign serves as a simple, practical foundation for activation-driven knowledge transfer and as a stepping stone toward precise, low-loss "brainwave" communication between models.